Stokes Space-Based Optical Modulation Format Recognition for Digital Coherent Receivers

Robert Borkowski, Darko Zibar, Antonio Caballero, Valeria Arlunno, and Idelfonso Tafur Monroy

***Abstract*— We present a technique for modulation format recognition for heterogeneous reconfigurable optical networks. The method is based on Stokes space signal representation and uses a variational Bayesian expectation maximization machine learning algorithm. Differentiation between diverse common coherent modulation formats is successfully demonstrated numerically and experimentally. The proposed method does not require training or a constellation diagram to operate, is insensitive to polarization mixing or frequency offset and can be implemented in any receiver capable of measuring Stokes parameters.**

***Index Terms*— Coherent detection, polarization multiplexing, modulation format recognition (MFR), modulation format detection (MFD), modulation format identification (MFI), Stokes space, Poincaré sphere, variational Bayesian expectation maximization (VBEM), Gaussian mixture models (GMM).**

I. Introduction

With the advent of reconfigurable transmitters capable of signal generation using arbitrary coherent optical modulation format [1], it is no longer possible to ensure that the receiver unit will know the incoming modulation format in advance. This paradigm change calls for a new receiver functionality. Modulation format recognition (MFR) [2] is essential to guarantee that signals, which are using diverse complex modulation formats, are optimally acquired and demodulated. This can be realized with software-defined receiver (SDR) provided that the modulation format is recognized before the crucial steps of signal processing. Modulation format must be known in order to enable operation of receiver algorithms that are modulation format opaque. An example of such a subsystem is decision directed equalization, where the knowledge of modulation format allows for superior error performance compared to blind equalization algorithm [3].

Latest reports in the field of digital signal processing (DSP) for coherent optical communication indicate that the next generation of receivers will implement Stokes space-based algorithms due their lower complexity or faster convergence. An advantage of Stokes space is that polarization mixing, carrier frequency offset and phase offset do not affect the 3-dimensional (3D) representation of the signal in the Poincaré sphere. Recently conceived Stokes space-based DSP include:

Manuscript received July 22, 2013; revised August 26, 2013; accepted September 9, 2013. Date of publication September 17, 2013; date of current version October 9, 2013. This work was supported by the Cognitive Heterogeneous Reconfigurable Optical Network project with funding from the EU FP7 Programme (FP7/2007-2013) under Grant 258644.

The authors are with DTU Fotonik, Department of Photonics Engineering, Technical University of Denmark, Kgs. Lyngby 2800, Denmark (e-mail: rbor@fotonik.dtu.dk; dazi@fotonik.dtu.dk; acaj@fotonik.dtu.dk; vaar@fotonik.dtu.dk; idtm@fotonik.dtu.dk).

Color versions of one or more of the figures in this letter are available online at http://ieeexplore.ieee.org.

Digital Object Identifier 10.1109/LPT.2013.2282303

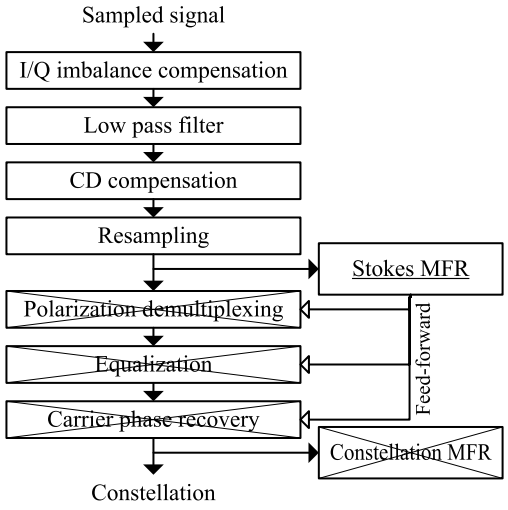

Fig. 1. DSP flow of a digital coherent receiver with the placement of Stokes MFR block. Crossed out blocks are not necessary to perform Stokes MFR. The location of constellation-based MFR [10] is shown for comparison.

polarization demultiplexing [4], [5], cross-polarization modulation compensation [6], PDL compensation [7] or OSNR monitoring [8].

Techniques for MFR have been well explored for wireless communications [9], and became widely used, e.g. in cognitive radio. In optical communication, this area has not been extensively investigated until very recently, mainly due to the static nature of fiber-optic networks. However, recently proposed cognitive optical networks architectures, such as CHRON [2], introduce reconfigurable and very dynamic networks where the receivers act autonomously and provide high degree of interoperability.

Literature lists four different methods that have been employed for optical MFR: i) monitoring from a constellation diagram with the use of k-means, which requires modulation transparent algorithms and entire receiver-side processing before MFR [10]; ii) artificial neural networks that need prior training [11]; iii) method based on signal cumulants [12]; iv) Stokes space and machine learning technique [13].

In this letter we expand upon our idea presented in [13]. By utilizing the DSP capabilities of a digital coherent receiver, we use Stokes space representation of the signal and employ a machine learning algorithm known as variational Bayesian expectation maximization (VBEM) [14] for Gaussian mixture models (GMM). The proposed method constitutes a major enhancement over the constellation analysis-based techniques, such as [10], as it allows for MFR at a considerably earlier stage in the receiver (cf. Fig. 1). The method does not require training, in contrast to neural network-based solution.

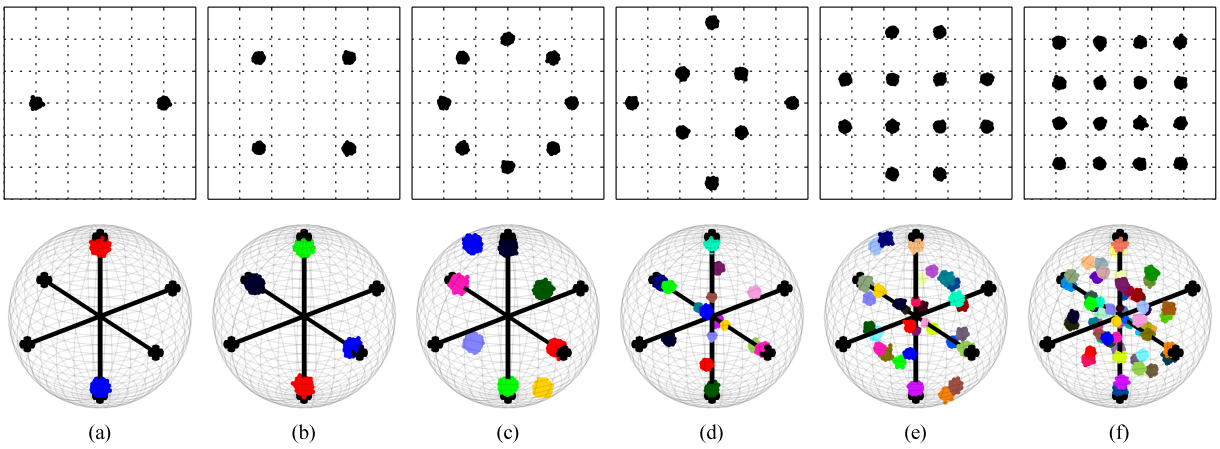

Fig. 2. Constellations (top row; only one polarization shown) and their corresponding Stokes space representation in the Poincaré (bottom row) for simulated data. (a) PDM BPSK, (b) PDM QPSK, (c) PDM 8-PSK, (d) PDM 8-QAM, (e) PDM 12-QAM, (f) PDM 16-QAM. Each color represents a separate cluster.

The information about recognized modulation format can be subsequently fed forward to the following DSP blocks to improve their performance. We report on successful optical modulation classification by discriminating from a possible set of BPSK, QPSK, 8-PSK, 8-QAM, 12-QAM and 16-QAM modulations.

II. Principles

A. Stokes Space Transformation and Representation

Stokes parameters are calculated from samples of the received signal as $S_0 = |x|^2 + |y|^2$, $S_1 = |x|^2 - |y|^2$, $S_2 = 2\Re(x\bar{y})$, $S_3 = 2\Im(x\bar{y})$. Three-vector (S_1, S_2, S_3) after normalization by $\max(S_0)$ determines location of received data points inside a 3D lens [4] in the Poincaré sphere. The transformation equations essentially operate on relative interpolarization signal powers and phase differences. Due to this, the transformed signal becomes independent of the polarization mixing, carrier frequency offset and phase offset. After the transformation, each considered modulation format is characterized by a different signature – number of clusters (clouds of points). Signatures of polarization-division multiplexed (PDM) modulation formats under consideration – {BPSK, QPSK, 8-PSK, 8-QAM, 12-QAM, 16-QAM} – are shown in Fig. 2. Those modulation formats result in, respectively, $N = \{2, 4, 8, 16, 32, 60\}$ clusters. We apply VBEM-GMM [15] machine learning algorithm to the Stokes space-transformed samples to determine the number of separate clusters, and hence modulation format. The reason for choosing this algorithm instead of e.g. k-means as in [10] is twofold: it allows for convenient detection of number of mixture components and behaves well with mixtures where per-cluster variances and intercluster distances vary, which is the case for Stokes MFR.

B. Per-Cluster Noise in Stokes Space

Assuming a random received data, in-phase (I) and quadrature components (Q) of both polarizations for every cluster are independent and identically distributed (i.i.d.) normal random variables (RV). Since signal transformation to Stokes space cancels out phase information, the deterministic phase component (phase offset) can be disregarded.

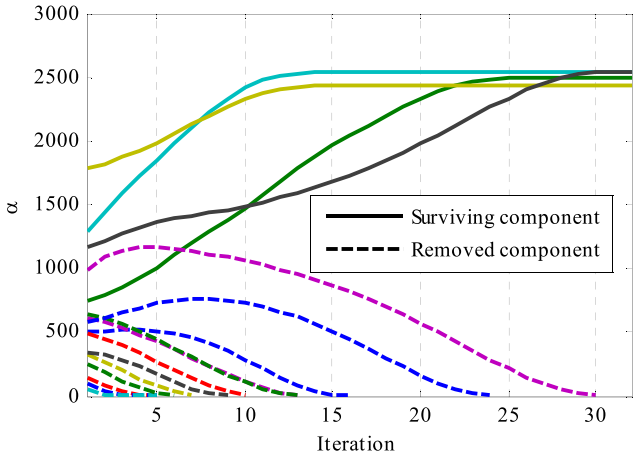

Fig. 3. Plot showing the value of α parameter for one VBEM-GMM run on simulated QPSK data. After the algorithm converges, only four components are left in the GMM, which is equivalent to four clusters in Stokes space, as shown in Fig. 2b.

The analytical evaluation of normally distributed variable after Stokes space transformation is very complex. However, by considering projections of per-cluster noise onto planes defined by normal unit vectors $\hat{S}_1$, $\hat{S}_2$ and $\hat{S}_3$ we find that $\hat{S}_1$ projection has a noncentral chi-squared (χ^2) distribution with 4 degrees of freedom while projections onto $\hat{S}_2$ and $\hat{S}_3$ have product-normal distributions.

C. Variational Bayesian Technique for Gaussian Mixture Models

Due to analytically intractable noise probability distribution functions for Stokes-transformed samples, we simplify our considerations by assuming that after Stokes transformation, the per-cluster noise is normally (Gaussian) distributed. Following that, we can reuse the general result from VBEM for GMM which has been well studied in literature [14].

The algorithm provides an iterative framework to optimize a set of parameters in a maximum likelihood (ML) sense.

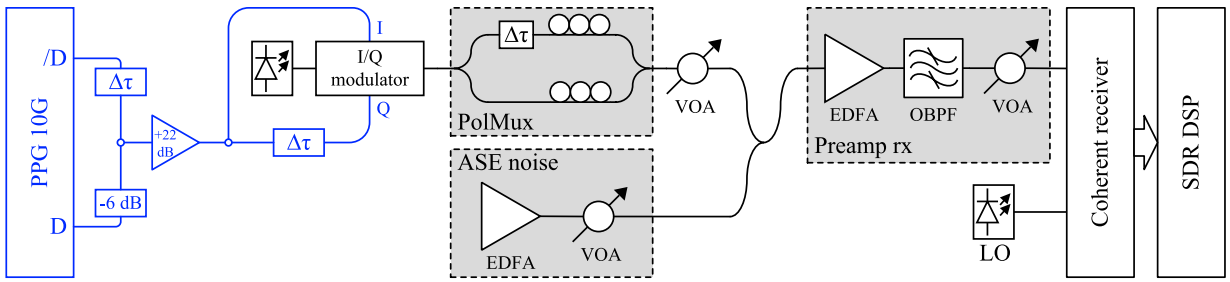

Fig. 4. Outline of the experimental setup. Blue - electrical subsystem, black - optical components. PPG - pulse pattern generator, $\Delta\tau$ - delay line (electrical or optical), I - in-phase, Q - quadrature, PolMux - polarization multiplexing stage, ASE noise - amplified spontaneous emission noise loading stage, EDFA - erbium-doped fiber amplifier, VOA - variable optical attenuator, Preamp rx - preamplified receiver, OBPF - optical bandpass filter, LO - local oscillator, SDR DSP - software defined receiver digital signal processing.

Since the assumed underlying distribution is GMM, the set of variables to optimize are distribution parameters. The procedure iterates over two steps: expectation (E step) and maximization (M step), similar to the ones presented in [16]. In E step, the current model parameters are used to assign observed data to mixture components. In M step the model parameters are updated based on the data assignment from the previous step. Those two steps are iteratively applied until convergence is achieved. An example of one run of VBEM-GMM algorithm is shown in Fig. 3. The model is initialized with a large number of components that well exceeds the largest number of points in the Stokes space among detectable modulation formats (60 for 16-QAM). Each curve in Fig. 3 represents one component and the value α (concentration parameter) for every component is proportional to the number of points in the Stokes space that belong to particular mixture component. The initial means for the GMM are chosen randomly from among the set of all points in the Poincaré sphere, as in general case the actual position of the lens in 3D space may be arbitrary [4], [7]. In order to reduce the necessary computational effort and thus speed up the algorithm, we introduce a modification where components with low α values are removed from the mixture. The number of surviving components, $\tilde{N}$, roughly equivalent to the number of clusters formed in the Stokes space, is then used to compute avalue of a simple cost function $j_N = |\tilde{N} - N|$. The cost function quantifies how close the detected number of clusters is to any of the considered modulation formats. The identification is done by finding $\min_N(j_N)$. It should be mentioned that $\tilde{N}$ is just an approximation of the actual number of clusters because of an assumption by which non-normal noise distributions are approximated by a GMM.

III. Simulation and Experiment Setup

A. Numerical Simulation

The numerical simulation of the modulation format recognition was performed by transmitting $10^4 \times \log_2 M$ points, where M is the modulation order, of a 10 Gbaud PDM signal through an additive white Gaussian noise channel. Noise power was varied for every modulation format to keep electrical signal-to-noise ratio (SNR) at 30 dB. Next, a carrier frequency offset and phase offset were applied. The signal was then passed through a set of DSP algorithms as shown in Fig. 1 and modulation format was recognized. The maximum number of iterations for the algorithm was set to 100. The convergence was monitored by evaluating the variational lower bound and the number of iterations typically did not exceed 50. Fig. 3 shows an example in which the convergence was achieved after 32 iterations. The last redundant component was removed in iteration 30, after which the number of components stabilized at 4, which corresponds to QPSK modulation format (cf. Fig. 2b).

B. Experimental Validation

The experimental setup, with a reconfigurable transmitter and receiver, capable of generation and reception of PDM 16-QAM and PDM QPSK at 10 Gbaud, is shown in Fig. 4. An optical I/Q modulator was provided with a carrier signal originating from a 100 kHz-linewidth laser operating at 1550.116 nm. Electrical inputs to the modulator were generated by a 10 Gb/s pulse pattern generator (PPG) with two dependent outputs (one negated). One of the outputs was delayed to assure decorrelation, the other one was attenuated by 6 dB, and both were combined in a resistive combiner. By toggling the state of one of the PPG outputs, the electrical signal was either 4- or 2-level. Next, the signal was amplified, divided in a resistive splitter, one of the branches was decorrelated and both were supplied as in-phase (I) and quadrature (Q) signals to the I/Q modulator. This resulted in, respectively, 16-QAM at 40 Gb/s or QPSK at 20 Gb/s in optical domain. Optical output of the I/Q modulator was subsequently polarization multiplexed to create PDM 16-QAM at 80 Gb/s or PDM QPSK at 40 Gb/s. The output of the polarization multiplexing stage was connected to amplified spontaneous emission (ASE) loading stage. For 16-QAM, an optical SNR of 27 dB was set, while 19 dB was used for QPSK experiment. The noisy signal was then preamplified, filtered by a 0.33 nm-broad optical bandpass filter (OBPF) to remove out-of-band ASE noise and attenuated with a variable optical attenuator (VOA) to clamp the power at the front-end of a coherent receiver to an optimal level. Another 100 kHz-linewidth laser, offset by several hundred MHz from the carrier wavelength was used as a local oscillator signal (LO) and supplied to the integrated coherent receiver. A 40 GSa/s, 13 GHz bandwidth oscilloscope was used to digitize electrical data output by the coherent receiver. The acquired traces were subsequently processed offline by a set of DSP algorithms outlined in Fig. 1. 8×10^4 points were used for Stokes MFR.

TABLE I

COST FUNCTION VALUE FOR SIMULATION AND EXPERIMENTAL CASES. RECOGNIZED MODULATION FORMATS WERE UNDERLINED

Cost function		Simulation						Exp.	
		PSK			QAM				
		2	4	8	8	12	16	QPSK	16QAM
PSK	2	0	2	6	14	30	58	2	48
	4	2	0	4	12	28	56	0	46
	8	6	4	0	8	24	52	4	42
QAM	8	14	12	8	0	16	44	12	34
	12	30	28	24	16	0	28	28	18
	16	58	56	52	44	28	0	56	10

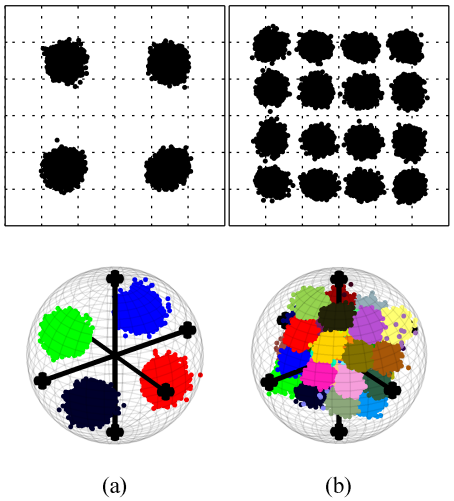

(a) (b)

Fig. 5. Constellations (top row; only one polarization shown) and their corresponding Stokes space representation in the Poincaré (bottom row) for experimental data. (a) PDM QPSK, (b) PDM 16-QAM.

IV. RESULTS

Top rows of Figs. 2 and 5 show one of the received signal polarizations, respectively for simulation and experiment, while bottom rows show Poincaré spheres with Stokes space representation of received signal. Each color in the Poincaré spheres represent separate cluster obtained after transformation.

The VBEM-GMM algorithm was used to count the number of clusters in the Stokes space and the cost function was calculated for every tested case. Table I presents the summary of results for both numerical simulation and experimental data. Every column corresponds to one case and the row indicates value of the cost function. For numerical simulation, lowest values of the cost function are located on the diagonal, indicating that recognition was successful in all investigated cases. Recognition was also successful for experimental data, with lowest values of cost function being associated with actual experimentally transmitted modulation formats.

V. SUMMARY

In this letter we reported on an optical modulation format recognition method from Stokes space parameters using variational Bayesian expectation maximization for Gaussian mixture models algorithm. This machine learning algorithm is used to count the number of clusters in Stokes space and provides an input to a cost function used to identify the modulation format. By using the Stokes space representation of the received signal, the method is insensitive to polarization mixing, carrier frequency offset and phase offset. Unlike previously published methods, it does not require training nor full set of coherent DSP algorithms to work. The method successfully recognized PDM BPSK, QPSK, 8-PSK, 8-QAM, 12-QAM and 16-QAM in numerical simulation as well as 16-QAM and QPSK from experimental data. The technique can be used in any receiver capable of measuring Stokes parameters, in particular digital coherent receivers. The recognized modulation format can be used as an additional information improving performance of follow-up DSP blocks of the digital coherent receiver.

REFERENCES

[1] K. Roberts and C. Laperle, "Flexible transceivers," in *Proc. ECOC*, 2012, pp. 1–3.

[2] I. T. Monroy, D. Zibar, N. G. Gonzalez, and R. Borkowski, "Cognitive heterogeneous reconfigurable optical networks (CHRON): Enabling technologies and techniques," in *Proc. 13th ICTON*, Jun. 2011, pp. 1–4.

[3] I. Fatadin, D. Ives, and S. J. Savory, "Blind equalization and carrier phase recovery in a 16-QAM optical coherent system," *J. Lightw. Technol.*, vol. 27, no. 15, pp. 3042–3049, Aug. 1, 2009.

[4] B. Szafraniec, B. Nebendahl, and T. Marshall, "Polarization demultiplexing in Stokes space," *Opt. Express*, vol. 18, no. 17, pp. 17928–17939, 2010.

[5] Z. Yu, *et al.*, "Polarization demultiplexing in Stokes space for coherent optical PDM-OFDM," *Opt. Express*, vol. 21, no. 2, pp. 3885–3890, 2013.

[6] P. Serena, A. Ghazisaeidi, and A. Bononi, "A new fast and blind cross-polarization modulation digital compensator," in *Proc. ECOC*, 2012, pp. 1–3, paper We.1.A.5.

[7] N. J. Muga and A. N. Pinto, "Digital PDL compensation in 3D Stokes space," *J. Lightw. Technol.*, vol. 31, no. 13, pp. 2122–2130, Jul. 1, 2013.

[8] T. Saida, *et al.*, "In-band OSNR monitor for DP-QPSK signal with high-speed integrated Stokes polarimeter," in *Proc. ECOC*, 2012, pp. 1–3.

[9] O. A. Dobre, A. Abdi, Y. Bar-Ness, and W. Su, "Survey of automatic modulation classification techniques: Classical approaches and new trends," *IET Commun.*, vol. 1, no. 2, pp. 137–156, Apr. 2007.

[10] N. G. Gonzalez, D. Zibar, and I. T. Monroy, "Cognitive digital receiver for burst mode phase modulated radio over fiber links," in *Proc. 36th ECOC*, Sep. 2010, pp. 1–3.

[11] F. N. Khan, Y. Zhou, A. P. Lau, and C. Lu, "Modulation format identification in heterogeneous fiber-optic networks using artificial neural networks," *Opt. Express*, vol. 20, no. 11, pp. 12422–12431, 2012.

[12] P. Isautier, A. Stark, K. Mehta, R. de Salvo, and S. E. Ralph, "Autonomous software-defined coherent optical receivers," in *Proc. OFC*, 2013, pp. 1–3, paper OTh3B.4.

[13] R. Borkowski, D. Zibar, A. Caballero, V. Arlunno, and I. T. Monroy, "Optical modulation format recognition in Stokes space for digital coherent receivers," in *Proc. OFC*, 2013, pp. 1–3, paper OTh3B.3.

[14] C. M. Bishop, "Approximate inference," in *Pattern Recognition and Machine Learning*, 3rd ed. New York, NY, USA: Springer-Verlag, 2006, ch. 10.

[15] M. Chen. (2012). *Variational Bayesian Inference for Gaussian Mixture Model* [Online]. Available: http://www.mathworks.com/matlabcentral/fileexchange/35362-variational-bayesian-inference-for-gaussian-mixture-model

[16] D. Zibar, *et al.*, "Nonlinear impairment compensation using expectation maximization for dispersion managed and unmanaged PDM 16-QAM transmission," *Opt. Express*, vol. 20, no. 26, pp. B181–B196, 2012.